Green-Synthesized Calcium Oxide Nanoparticles for Adsorption, Antibacterial Applications, and Alleviating Water Stress in Fenugreek

Waleed Khalid Mahdi[1], Hassan Abdul Razaq Ali [2], Aqeel Oudah Flayyih[3], Falih Hassan Musa[4] and Ahmed Saleem Otaiwi[5]

[1]*Department of Chemistry, College of Education for Pure Science - Ibn Al-Haitham, University of Baghdad, 00964 Baghdad, Iraq*

[2]*Biology Department, College of Science, Mustansiriyah University, 00964 Baghdad, Iraq*

[3]*Chemistry Teacher, Ministry of Education, 00964 Baghdad, Iraq*

[4]*Dean of College of Health and Medical Technology, Ashur University, 00964 Baghdad, Iraq*

[5]*Researcher Chemist, Ministry of Water Resources, 00964 Baghdad, Iraq*

waleed.k.m@ihcoedu.uobaghdad.edu.iq,hassanalsady962@uomustansiriyah.edu.iq, oqil.awda1205a@ihcoedu.uobaghdad.edu.iq,falih.hassan@au.edu.iq,ahmedrawe@hotmaiol.com

Keywords: Green Synthesis, Caonps, Antibacterial, Adsorbent, Fenugreek.

Abstract: In this research, a novel synthesis of CaONPs has been developed via an environmentally friendly, green method. Garlic extract (Allium sativum) was used as a green-reducing and stabilizing agent for CaONPs. The average particle size of CaONPs was approximately 24.42 nm. The synthesized CaONPs were identified by using Fourier transform infrared (FT-IR) spectroscopy, U.V.-vis spectrum, X-ray diffraction (XRD), Field Emission-Scanning Electron Microscopy (FE-SEM), Transmission Electron Microscopy, transmission electron microscopy (TEM), Energy Dispersive X-ray spectroscopy (EDX), Atomic Force Microscopy (AFM), and zeta potential (Zp) analysis. The current study highlights the notable applications for CaONPs. First, an antimicrobial assay revealed a high antibacterial and antifungal activity, with the maximum zone of inhibition observed at different concentrations of CaONPs. Secondly, adsorbent for CaONPs in an aqueous solution containing M^{+2} ions (Co, Ni, Cu). The removal percentages (R%) were Co (II) 93.47%, Ni (II) 87.58%, and Cu (II) 88.53%. Thirdly, the study of fenugreek under water stress revealed that CaO-NPs positively enhance water stress tolerance.

1 INTRODUCTION

Green synthesis protocols used for synthesizing (MONPs) have become recently drawn the attention of researchers due to their lower cost, greater credibility, and simplicity [1], [2]. CaONPs are safe, non-toxic, environmentally friendly, and have a high reputation across all elements because of their stability [3]. Different sizes of CaONPs have been synthesized using plant materials such as the leaves of Trigon sp., which yielded nanoparticles with an average size of 51.64 nm [4]. Piper nigrum with 47.08 nm [5], Moringa oleifera with 32.08 nm [6], and Pistacia Atlantica with sizes ranging from 40-130 nm [7].

Nanotechnology has demonstrated the potent antibacterial capabilities of metal oxide nanoparticles (MONPs) [8]. Similarity investigations have illustrated the antibacterial activities of metal oxide nanoparticles [9], [10], [11]. Nanoparticles are commonly employed in wastewater treatment due to their large surface area and small size, which confer strong adsorption reactivity and capacity [12], [13]. Moreover, MONPs have been extensively utilized in agriculture to mitigate water stress, playing crucial roles in signaling pathways, defense metabolism, and regulatory activities [14], [15]. In this study, we established protocols for the green synthesis of CaONPs using garlic extract. The synthesized CaONPs were evaluated for their applications, including their efficiency as adsorbents for removing Co (II), Ni (II), and Cu (II) from aqueous solutions, and their effect on antibacterial activity. Additionally, we investigated the impact of CaONPs on enhancing fenugreek's (Trigonella foenum-graecum L.) resistance to water stress.

The use of plant-based extracts for the synthesis of nanoparticles is an emerging area of interest due to its sustainable and eco-friendly approach. Garlic extract, in particular, has been recognized for its rich bioactive compounds, which can act as reducing and stabilizing agents in nanoparticle synthesis [16]. This method not only reduces the need for hazardous chemicals but also aligns with the principles of green chemistry. Furthermore, the adsorption properties of CaONPs were analyzed to determine their effectiveness in removing heavy metal ions from wastewater.

This application is particularly relative given the growing concerns about water pollution and the need for efficient and cost-effective treatment methods. The antimicrobial properties of CaONPs were also examined, providing insights into their potential use in medical and agricultural settings. Finally, the study explored the role of CaONPs in enhancing the water stress tolerance of fenugreek plants. This aspect is crucial for developing strategies to improve crop resilience under drought conditions, which is a significant challenge in agriculture today. By integrating nanotechnology with botany, this research contributes to the development of innovative solutions for sustainable agriculture and environmental management.

2 MATERIALS TECHNIQUES AND METHODS

2.1 Sample Collection

Deionized water (DI) was obtained from the Chemical Lab, College of Education for Pure Science / Ibn Al-Haitham - University of Baghdad. Cobalt sulphate $CoSO_4$, copper sulphate pentahydrate $CuSO_4 \cdot 5H_2O$, nickel sulphate heptahydrate $NiSO_4 \cdot 7H_2O$, calcium sulphate $CaSO_4$, and sodium hydroxide NaOH were purchased from Merck, Germany. All chemicals were used without further purification. Garlic was sourced from the local market in Baghdad, Iraq. Fresh garlic bulbs were cleaned with water to get rid of dust, peels, and other contaminants, then dried at 37 ^oC and grated to facilitate extraction. A 500 mL beaker was filled with 20 g of garlic and 200 mL of deionized water. The mixture was heated to 80 ^oC with continuous stirring for 30 min. After cooling to room temperature, the yellowish mixture was filtered to remove impurities. The filtrate was then centrifuged at 4000 rpm for 15 min to eliminate any remaining fine suspended materials.

2.2 CaONPs Preparation by Garlic Extract with CaSO4

Calcium Sulphate $CaSO_4$ 4g was dissolved in 100 mL of deionized water at a concentration of 0.1M in a beaker with a volume of 500 mL, to which 100 mL of garlic fruit extract that had previously been prepared gradually at a temperature of 90 ^oC was added with continuous stirring, gradually add drop by drop a solution of sodium hydroxide with a concentration of 1M through the dissolution of 2 g of NaOH in 50 mL of deionized water until the pH reaches 12. The solution was left for 48 h, to form a light brown precipitate. The precipitate was separated using a centrifuge (4000 – 4500 rpm), then filtered and washed with deionized water and hot ethanol. after that it was dried by using an electric oven at a temperature of 300 ^oC for 15h, leaving a white powder as shown in Figure 1.

2.3 Instrumentation Techniques

An electronic balance (A 220/C/1 model), PLC centrifuge (4000 – 4500 rpm, FAITHFUL), electric oven, water bath with shaking (SCL F), pH tape, and a UV-Vis spectrophotometer (160/UV, Shimadzu) were utilized in this study. The FT-IR studies were conducted using a Shimadzu 8500S spectrometer in the range of 400 – 4000 cm-1 at Baghdad University. (XRD) analysis was performed using a Holland/Phillips system at the laboratory center of Baghdad. (FE-SEM) was carried out using a 300 Hv system (Germany-Z. S). Energy (EDX) and (TEM) (EMIOC-100Kv, Germany) were conducted at Kashan University, Iran. (AFM) (Nano surf AG. Liestal, Switzerland) was performed at the College of Science/ University of Baghdad, and Zeta potential measurements (14011201, Mahamax – 45184- Zeta-03 nzt) were also conducted at Kashan University, Iran. Two reference bacteria, Staphylococcus aureus (G+) and Escherichia coli (G-), were used to examine the synthesized CaONPs, as well as the fungal species Candida albicans, using the diffusion method and nutrient media, including Mueller Hinton Agar (MHA) and Potato Dextrose Agar (PDA).

2.4 Types of Bacteria and Fungi

Two strains of bacteria and one fungal species were used in the studies: Gram-negative Escherichia coli, Gram-positive Staphylococcus aureus, and the fungal species Candida albicans. The disc diffusion method was performed using nutrient media, specifically, Mueller Hinton Agar (MHA) for bacterial studies, and the same method was applied

for antifungal activity. The CaONPs were prepared using garlic extract and tested at different concentrations, ranging from 2 to 0.25 mg/mL.

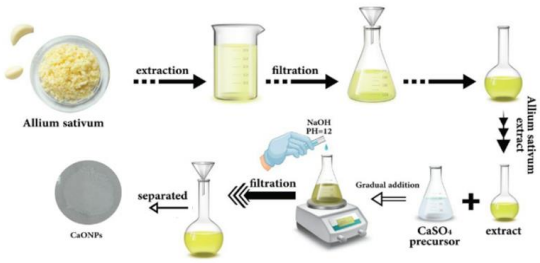

Figure 1: Preparation steps of CaONPs using garlic extract.

2.5 Adsorption Studies

In this study, the effect of metal ions (II) such as Co, Ni, and Cu on CaONPs showed promising results. $CoSO_4$, $NiSO_4 \cdot 7H2O$, and $CuSO_4 \cdot 5H_2O$ were used as the sources of these ions, each at a concentration of 12.5 mg/L. In each experiment, 0.1 g of CaONPs was mixed with 12.5 mg/L of each metal ion in a tube and agitated using a shaker water bath at 35 ºC with a rate of 120 rpm and pH 6. The initial concentrations of ($M^{(II)}$: Co, Ni, and Cu) were taken from synthetic metal ion solutions. After adsorption, the samples were filtered by centrifugation, and the liquid was analyzed for these metal ions using a UV-visible spectrophotometer.

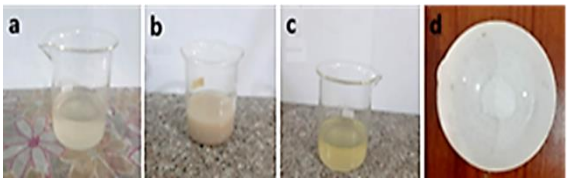

Figure 2: Color change solutions of CaSO4 and bio-redactor of Garlic (Allium Sativum) extract a) Turbid, b) Milky, c) Pale yellow, and d) CaONPs powder.

The experimental design layout was applied in the execution of each experiment. The formula was used to calculate the adsorbent's removal efficiency, or

$$R\%. [17, 18]. R\% = \frac{100 (Co - Ct)}{Co}. \quad (1)$$

Where Co and Ct (mg /L) are the initial concentration and concentration at time 10-80 min. R: represents the percentage of adsorption of nickel, copper, and cobalt ions.

2.6 Pots Experiment

The experiment was performed as a factorial experiment in a plastic house belonging to the Biology Department, College of Science, Al-Mustansiriyah University. The study aimed to reduce the adverse effects of water stress, represented by three irrigation periods, on the fenugreek crop using different concentrations of calcium oxide nanoparticles (CaONPs). Ten seeds were germinated in plastic pots containing 5 kg of soil, and the harvest was taken 70 days after planting to study vegetative growth, yield, and some antioxidant concentrations. The treatments included T1 (5-day irrigation period), T2 (10-day irrigation period), T3 (15-day irrigation period), T4 (T1 + 50 mg/L CaONPs), T5 (T1 + 100 mg/L CaONPs), T6 (T2 + 50 mg/L CaONPs), T7 (T2 + 100 mg/L CaONPs), T8 (T3 + 50 mg/L CaO NPs), and T9 (T3 + 100 mg/L CaONPs).

The parameters studied were plant weight (cm), dry weight (g), number of pods, seed weight (g), proline concentration (µg/g) [19] salicylic acid (SA) concentration (µg/mL) [20], ascorbic acid (ASA) concentration (mg/100g) [21], and α-tocopherol (α-TOC) concentration (µg/g) [22]. Three replicates were used in a completely randomized design (CRD), and the least significant difference (LSD) test was utilized to statistically evaluate the data at a 5% probability level [23].

3 RESULT AND DISCUSSION

An aqueous extract of garlic was used with CaSO4. The changing color of the solutions is shown in Figure 2. Initially, the solution was turbid Figure 2a, which then turned milky Figure 2b, and subsequently became pale yellow Figure 2c. The final product was a white powder of CaONPs Figure 2d.

3.1 FT-IR Spectroscopy

FT-IR was used to identify CaONPs as shown in Figure 3. Peaks located at 540.07, 497.64, and 466.78 cm^{-1}, confirming the formation of CaONPs [6]. Peaks were observed at 659.66 and 567.08 cm-1 for A. sativum crude extract [24].

3.2 UV-Visible Absorption Spectroscopy Analysis

UV-vis spectrum confirmed the presence of CaONps as shown in Figure 4 at 248nm. The following

equation was used to determine the energy gap band. Eg = 1239.83 / λ. Lambadi peak absorption is represented λ, and the bulk band, Eg, is given in eV as follows: Eg = 1239.83 / 248 = 4.99 eV [25], [26].

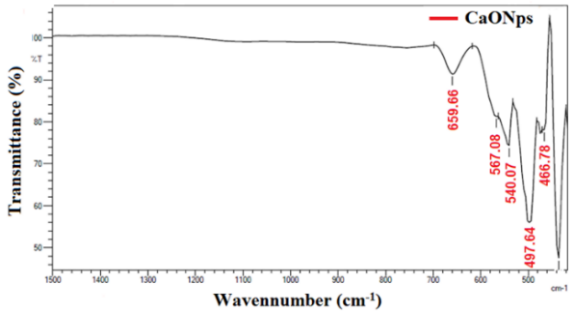

Figure 3: FT – IR spectrum of CaONPs.

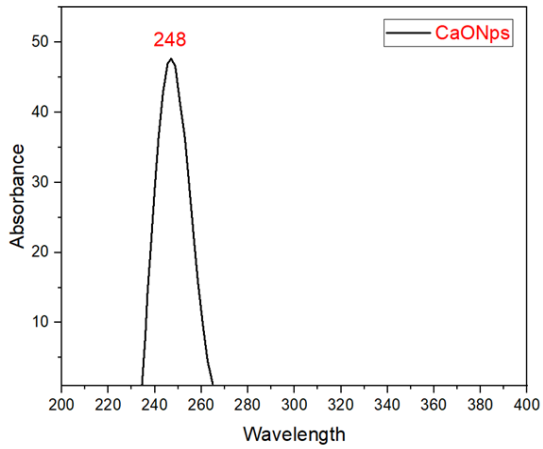

Figure 4: UV-vis spectrum of CaONPs.

3.3 X-Ray Diffraction

Further proof of the product CaONPs over the diffraction angle (2θ) range of 20° - 80°. Figure 5 shows the peaks observed at 2θ = 38.74° (111), 42.99° (200), 63.12° (220), 75.32° (311), and 80° (222). The average size (D) of the synthesized CaONPs was determined to be 24.42 nm by applying the Scherrer equation to measure the crystallite size. The polycrystalline and monophasic cubic structure of CaONPs, as character by the XRD pattern, is revealed by the sharp peaks. The crystal structures and the provided JCPDS data (JCPDS powder diffraction data card No. 77-2376) are in good agreement. Miller indices are shown in Table 1. The diffraction peaks' line broadening suggests that the CaONps are in the nanometer range. The products had good crystallinity, as evidenced by the distinctive peaks' lower spectral width and higher intensity. The final results of synthesized products are high-quality CaONps, as indicated by the absence of peaks related to contaminants [27].

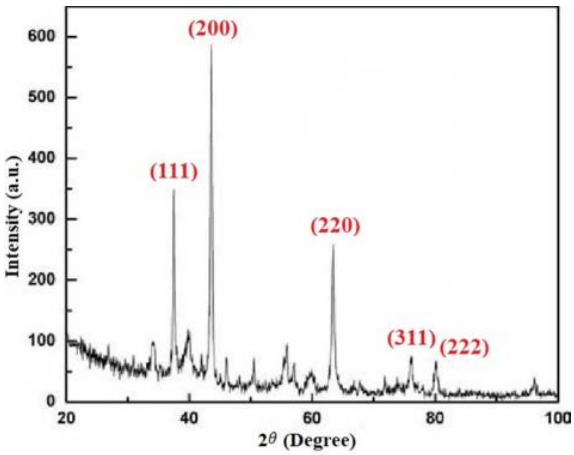

Figure 5: XRD pattern of CaONPs.

Table 1: Summary of XRD data analysis for CaONPs.

Pos. [°2θ]	Height [cts]	FWH-M [°2θ]	d-spacing [Å]	Tip width [°2θ]	Matched by
38.74	644.9	0.29	2.32	0.35	29.81
42.49	712.7	0.34	2.12	0.41	25.86
63.12	210.4	0.39	1.47	0.47	24.75
75.32	250.5	0.39	1.26	0.47	26.65
79.94	208.4	0.72	1.23	0.86	15.05

3.4 Morphological Study

FE-SEM and TEM images are shown in Figure 6, and Figure 7, respectively. In the FE-SEM images of CaONps, a variety of shapes such as tubes, cubes, and flowers, with several spaces between nanoparticles were observed. The mean size of the particles is 24.20 nm. This represents the size and morphology of the synthesized CaONPs [28].

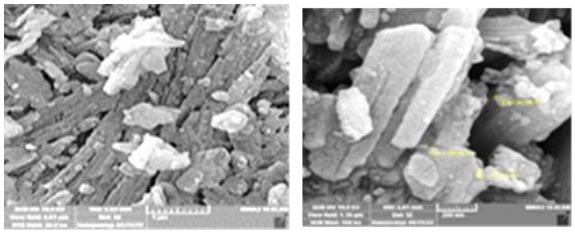

Figure 6: FE-SEM image of CaONPs.

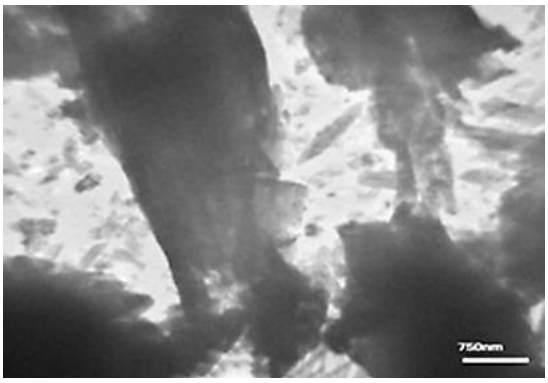

Figure 7: TEM image of CaONPs.

3.5 Energy Dispersive X-Ray Spectroscopy

In general, EDX is used to identify the chemical composition, as shown in Figure 8. The EDX spectrum of CaONPs showed a strong peak for calcium and a medium peak for oxygen, proving that there are no observable impurities in the calcium, which indicates it is chemically pure. The presence of Au is also confirmed by the EDX, which may have resulted from the usage of the standard and sample preparation for SEM-EDX analysis. [29].

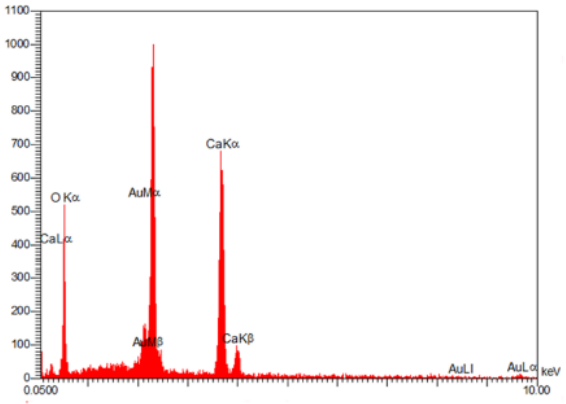

Figure 8: EDX composition spectrum of CaONPs.

3.6 Atomic Force Microscopy

The AFM offers visualization and analysis in three dimensions, revealing that the nanoparticles' size is in good identical to the data obtained from FE-SEM and TEM. The AFM histogram and statistical particle analysis of CaONPs powder with topography parameters, and 3D AFM images of the nanoparticles indicating the pyramid-like grains are presented in (Figure 9, and Figure10) [30] .

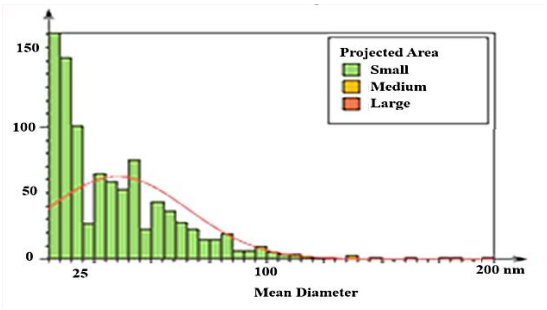

Figure 9: AFM histogram and statistical particle analysis of CaONPs powder.

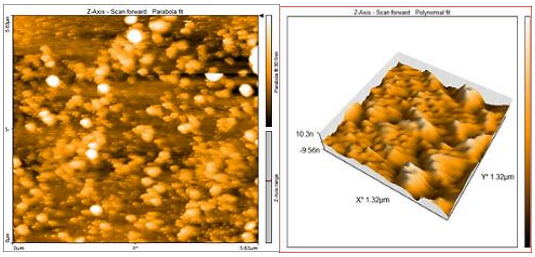

Figure 10: 3D AFM surface structure images of CaONPs.

3.7 Zeta Potential of CaONPs

Figure 11, depicts, the Zeta potential of CaONPs, with a value of -20.5 mV ± 2.3 mV. The high level of stability values of the CaONPs produced are highly charged particles, indicated by the high zeta potential values, which in turn prevents aggregation and agglomeration due to their large repulsion force [31].

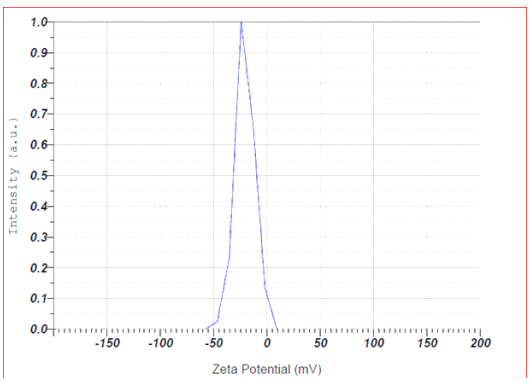

Figure 11: Zeta potential values of CaONPs.

3.8 Antibacterial Study

Using the agar well diffusion method, the antibacterial effectiveness of CaONPs was assessed against Escherichia coli, Staphylococcus aureus, and the fungal species Candida albicans. The outcomes

show that the HCl dilution negative control did not exhibit an inhibition zone, indicating that the control in its natural state, devoid of nanoparticles, exhibited no antibacterial activity. When the concentrations of the CaONPs sample (A) were 2, 1, 0.5, and 0.25 mg/mL, it was found out that at all these concentrations, the CaO nanoparticles caused a growth delay in all microorganisms. Higher antibacterial activity was observed in the range of 35 – 39 mm at different concentrations from 2 to 0.25 mg/ml [32]. All these results and the diameters of the inhibition zones are represented in Table 2.

Table 2: Shows the diameters of the inhibition zones in mm of CaONPs sample in different concentrations.

CaONPs Sample	D1	D2	D3	D4
Concentration	2mg/mL	1mg/mL	0.5mg/mL	0.25mg/mL
Micro organisms' type	Diameter of inhibition zone (mm)			
S.auras	39	37	38	35
E. Coli	35	32	31	28
C. albicans	25	22	19	17

3.9 Adsorption Study

According to the results, CaONPs demonstrated effective removal of various divalent metal ions, specifically cobalt, nickel, and copper, from a solution of distilled water, as shown in Figure 12. The percentage of ions removed by CaONPs decreased from 95.90%, 87.33%, and 89.02% after 10 min to 91.86%, 86.92%, and 88.40%, respectively, indicating the number of active sites available on CaONPs. During the first 80 min of the adsorption process, the sites on CaONPs gradually became saturated. The removal efficiencies (R%) for the divalent metal ions of cobalt, nickel, and copper were higher, with values of 93.47%, 87.58%, and 88.53%, respectively [33].

3.10 Study of The Impact of Water Stress on The Growth of Fenugreek at Current CaONPs Concentrations

The results in Table 3, shows a significant effect of (irrigation periods) and water stress on reduced plant height, dry weight, number of pods, and seed weight. When spacing irrigation periods from 5 days (T1) to 15 days (T3), these parameters decreased by 27.95%, 55.61%, 59.26%, and 37.67%, respectively. Furthermore, CaONP spraying mitigated the harmful effects of water stress by increasing the vegetative growth parameters and yield contents mentioned above. Specifically, in the T3 treatment, the usage of (50 mg/L of CaONPs) (T8) resulted in significant increases of 15.60%, 62.63%, 63.64%, and 28.76%, respectively. Additionally, the usage of (100 mg/L of CaONPs) (T9) rendered in significant increases of 23.93%, 68.69%, 54.55%, and 37.73%, respectively.

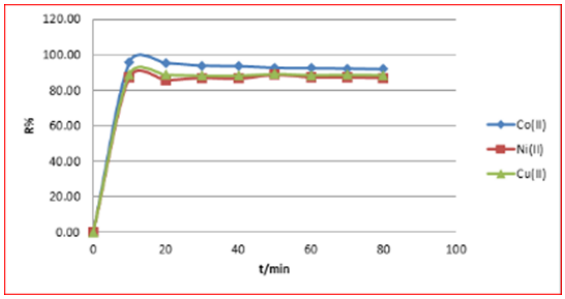

Figure 12: Represented of adsorption of cobalt, nickel, and copper metal ions with CaONPs, garlic extract, and calcium sulphate.

Table 3: Effect of water stress and CaONPs on vegetative growth and yield of fenugreek.

Treat.	Plant height (cm)	Dry weight (g)	Pods No.(pod)	Seeds weight (g)
T1	38.97	2.23	13.50	6.08
T2	30.62	1.47	7.50	4.28
T3	28.08	0.99	5.50	3.79
T4	41.56	2.45	15.50	6.40
T5	43.94	2.68	16.50	6.79
T6	36.98	1.84	9.50	5.79
T7	37.26	2.15	12.00	5.92
T8	32.46	1.51	9.00	4.88
T9	34.80	1.67	8.50	5.22
LSD (0.05)	1.70	0.27	1.63	0.18

The results in Table 4, showed an increase in antioxidant concentration with increasing water stress. The T3 treatment yielded high values of proline, salicylic acid, ascorbic acid, and α-tocopherol, with rates of 172.47%, 161.75%, 62.44%, and 64.85%, respectively, compared to the T1 treatment (control). When CaONPs were sprayed, there was a significant decrease in the average antioxidant concentrations mentioned above, especially in the T3 treatment. The usage of (50 mg/L of CaO NPs) (T8) resulted in significant

decreases of 35.87%, 44.14%, 16.69%, and 17.87%, respectively. Similarly, the usage of (100 mg/L of CaONPs) (T9) resulted in significant decreases of 50.97%, 53.88%, 22.34%, and 35.59%, respectively.

Table 4: Effect of water stress and CaONPs on antioxidants.

Treat.	Proline (µg.g-1)	Salicylic acid (µg.ml-1)	Ascorbic acid (mg.100g-1)	α-tocopherol (µg.g-1)
T1	3.96	2.51	55.75	42.10
T2	8.41	4.35	80.28	60.50
T3	10.79	6.57	90.56	69.40
T4	2.19	1.47	50.29	37.90
T5	1.98	1.20	42.52	34.20
T6	4.98	2.75	64.53	49.70
T7	3.19	2.52	62.47	44.40
T8	6.92	3.67	75.45	57.00
T9	5.29	3.03	70.33	44.70
LSD (0.05)	0.77	0.66	3.45	9.92

Drought is an environmental factor that decreases plant growth and yield. Many studies have shown that drought negatively affects morphological growth (plant height, leaf area, root development, branch number, and biomass accumulation), metabolic processes (photosynthesis and respiration), and productivity [34]. The reduction in morphological and physiological characteristics and yield may be due to a decrease in water content in plant tissues, reduced leaf area and chlorophyll concentration, and ultimately a decreased photosynthetic rate and protein synthesis [35]. Furthermore, drought can alter the plant's CO_2 metabolism by decreasing Rubisco inactivation, RuBP regeneration, and stomata open system [36]. Recent studies have shown that water deficits in plant tissues reduce yield by affecting flowering time and causing pollen grain sterility [37]. In addition, water stress increases reactive oxygen species (ROS) and accumulates proline in cells [38].

Plants respond by producing secondary compounds like phenols and stimulating enzymatic and non-enzymatic antioxidants to scavenge ROS [39]. Nanoparticles (NPs) enhance the effectiveness of the antioxidant system in different plants by reducing ROS in plant tissues or increasing the concentration of photosynthetic pigments (anthocyanins and β-carotene) to improve growth and yield. Moreover, NPs can alter metabolism beyond the physiological and biochemical levels, potentially inducing the gene expression of antioxidant biosynthesis [40].

In this research, CaONPs played a positive role in water stress tolerance by enhancing morphological growth, resulting in greater plant height, dry weight, and improved yield content. Foliar application of CaO ameliorated the harmful effects of drought by enhancing proline accumulation and reducing antioxidant concentrations (SA, ASA, and α-TOC). Additionally, CaONPs positively affected plant growth at morphological, physiological, biochemical, and molecular levels, thereby increasing drought stress tolerance [41].

4 CONCLUSIONS

Allium sativum (garlic extract) has been successfully used to synthesize CaONps via the biosynthesis method. FT-IR and UV-visible spectra confirmed the presence of CaO bonds, with a peak centered at 245 nm and an energy gap (Eg) of 4.99 eV. XRD analysis of CaONPs shows a monophasic cubic structure with an average crystallite size of 24.42 nm. FE-SEM and TEM images reveal a variety of shapes, such as tubes, cubes, and flowers. EDX peaks indicate the presence of Ca and O peaks. AFM provides 3D images of nanoparticles, showing pyramid-like grains indicative of the presence of CaONPs. The Zeta potential value of -20.5 mV indicates highly charged particles.

CaONPs demonstrated antimicrobial activity, with inhibition zones ranging from 25 to 39 mm, indicating strong inhibition against the growth of *S. aureus*, *E. coli*, and the fungal species *Candida albicans.* CaONPs effectively removed Co (II), Ni (II), and Cu (II) from aqueous solutions, with yields of 95.90%, 87.33%, and 89.02% after 10 min, and 91.86%, 86.92%, and 88.40% after 80 min, respectively. The adsorption efficiencies (R%) were 93.47%, 87.58%, and 88.53%, respectively. The study of water stress in fenugreek (Trigonella foenum-graecum L.) shows that CaONPs have positive growth-promoting effects on the growth of fenugreek.

ACKNOWLEDGMENTS

To University of Ashur / College of Health and Medical Technology, and College of Education of Pure Science, Ibn- Al Haitham / Department of Chemistry- University of Baghdad / Iraq. For support.

REFERENCES

[1] P. Khandel, R. K. Yadaw, D. K. Soni, L. Kanwar, and S. K. Shahi, "Biogenesis of metal nanoparticles and their pharmacological applications: present status and application prospects," Journal of the Iranian Chemical Society, 2018, doi: 10.1007/s40097-018-0267-4.

[2] M. Y. Al-darwesh, S. S. Ibrahim, and M. A. Mohammed, "A review on plant extract mediated green synthesis of zinc oxide nanoparticles and their biomedical applications," Results in Chemistry, 2024, doi: 10.1016/j.rechem.2024.101368.

[3] T. Pagar, S. Ghotekar, S. Pansambal, R. Oza, and B. P. Marasini, "Facile plant extract mediated eco-benevolent synthesis and recent applications of CaO-NPs: a state-of-the-art review," Journal of Chemical Reviews, 2020, doi: 10.22034/jcr.2020.107355.

[4] B. Maringgal, N. Hashim, I. S. M. A. Tawakkal, M. H. Hamzah, and M. T. M. Mohamed, "Biosynthesis of CaO nanoparticles using Trigona sp. honey: physicochemical characterization, antifungal activity, and cytotoxicity properties," Journal of Materials Research and Technology, vol. 9, no. 5, 2020, doi: 10.1016/j.jmrt.2020.08.054.

[5] M. Mushtaq, S. M. Hassan, and S. S. Mughal, "Synthesis, characterization and biological approach of nano oxides of calcium by Piper nigrum," American Journal of Chemical Engineering, vol. 10, no. 4, 2022.

[6] V. Jadhav et al., "Green synthesized calcium oxide nanoparticles (CaO NPs) using leaves aqueous extract of Moringa oleifera and evaluation of their antibacterial activities," Journal of Nanomaterials, vol. 2022, 2022, doi: 10.1155/2022/9047507.

[7] M. H. Meshkatalsadat and M. Solaimani, "Facile and eco-friendly method for synthesis of calcium oxide nanoparticles utilizing Pistacia atlantica leaf extracts and its characterization," International Journal of New Chemistry, vol. 10, no. 1, 2023.

[8] M. Alavi, S. Dehestaniathar, S. Mohammadi, A. Maleki, and N. Karimi, "Antibacterial activities of phytofabricated ZnO and CuO NPs by Mentha pulegium leaf/flower mixture extract against antibiotic resistant bacteria," Advanced Pharmaceutical Bulletin, vol. 11, no. 3, 2021, doi: 10.34172/apb.2021.057.

[9] M. J. Mohammed, W. K. Mahdi, and F. H. Musa, "Green synthesis, characterization, and biological activity of zinc oxide nanoparticles using aqueous extract of Beta vulgaris and the seed of Abrus precatorius," International Journal of Drug Delivery Technology, vol. 11, no. 3, 2021, doi: 10.25258/ijddt.11.3.56.

[10] M. Y. Al-darwesh, S. S. Ibrahim, M. F. Naief, A. M. Mohammed, and H. Chebbi, "Synthesis and characterizations of zinc oxide nanoparticles and its ability to detect O_2 and NH_3 gases," Results in Chemistry, vol. 6, 2023, doi: 10.1016/j.rechem.2023.101064.

[11] Y. Zhan et al., "Therapeutic strategies for drug-resistant Pseudomonas aeruginosa: metal and metal oxide nanoparticles," Journal of Biomedical Materials Research Part A, 2024, doi: 10.1002/jbm.a.37677.

[12] K. A. Altammar, "A review on nanoparticles: characteristics, synthesis, applications, and challenges," Frontiers in Microbiology, 2023, doi: 10.3389/fmicb.2023.1155622.

[13] H. M. Abuzeid, C. M. Julien, L. Zhu, and A. M. Hashem, "Green synthesis of nanoparticles and their energy storage, environmental, and biomedical applications," Crystals, vol. 13, no. 11, 2023, doi: 10.3390/cryst13111576.

[14] H. K. Chandrashekar et al., "Nanoparticle-mediated amelioration of drought stress in plants: a systematic review," 3 Biotech, 2023, doi: 10.1007/s13205-023-03751-4.

[15] M. F. Seleiman et al., "Drought stress impacts on plants and different approaches to alleviate its adverse effects," Plants, vol. 10, no. 2, 2021, doi: 10.3390/plants10020259.

[16] A. Shang et al., "Bioactive compounds and biological functions of garlic (Allium sativum L.)," Foods, vol. 8, no. 7, 2019, doi: 10.3390/foods8070246.

[17] B. S. Maharani, "Synthesis and characterization of calcium oxide nanoparticles and their application in the adsorption of indigo carmine," Jurnal Kartika Kimia, vol. 7, no. 1, 2024, doi: 10.26874/jkk.v7i1.253.

[18] R. Kasirajan, A. Bekele, and E. Girma, "Adsorption of lead (Pb-II) using CaO-NPs synthesized by sol-gel process from hen eggshell: response surface methodology for modeling, optimization and kinetic studies," South African Journal of Chemical Engineering, vol. 40, 2022, doi: 10.1016/j.sajce.2022.03.008.

[19] B. F. Alowaiesh, A. B. El-Mansy, D. A. El-Alakmy, E. A. Rehema, and D. A. El-Moneim, "Biochemical, physiological, and molecular responses of diverse olive cultivars to different irrigation regimes," Notulae Botanicae Horti Agrobotanici Cluj-Napoca, vol. 51, no. 4, 2023, doi: 10.15835/NBHA51413395.

[20] M. Shahbaz et al., "Mitigation of salinity stress in sunflower plants (Helianthus annuus L.) through topical application of salicylic acid and silver nanoparticles," Physiology and Molecular Biology of Plants, vol. 31, no. 1, pp. 27–40, 2025, doi: 10.1007/s12298-024-01535-5.

[21] M. Maleki, A. Shojaeiyan, and A. Mokhtassi-Bidgoli, "Differential responses of two fenugreek (Trigonella foenum-graecum L.) landraces pretreated with melatonin to prolonged drought stress and subsequent recovery," BMC Plant Biology, vol. 24, no. 1, 2024, doi: 10.1186/s12870-024-04835-w.

[22] H. B. Rashmi and P. S. Negi, "Chemistry and physiology of fruits and vegetables," in Advances in Food Chemistry: Food Components, Processing and Preservation, 2022, doi: 10.1007/978-981-19-4796-4_12.

[23] G. S. Al-Hadithi, N. Faleh, and H. A. A. Al-Saady, "Effect of different fertilizers on growth and nutrient state of fenugreek (Trigonella foenum–graecum L.)," Bionatura, vol. 8, no. 1, 2023, doi: 10.21931/RB/CSS/S2023.08.01.27.

[24] J. M. M. Mohamed et al., "Superfast synthesis of stabilized silver nanoparticles using aqueous Allium sativum (garlic) extract and isoniazid hydrazide conjugates: molecular docking and in-vitro characterizations," Molecules, vol. 27, no. 1, 2022, doi: 10.3390/molecules27010110.

[25] A. Haider et al., "Green synthesized phytochemically (Zingiber officinale and Allium sativum) reduced nickel oxide nanoparticles confirmed bactericidal and catalytic potential," Nanoscale Research Letters, vol. 15, no. 1, 2020, doi: 10.1186/s11671-020-3283-5.

[26] T. S. S. K. Naik et al., "Green and sustainable synthesis of CaO nanoparticles: its solicitation as a sensor material and electrochemical detection of urea," Scientific Reports, vol. 13, no. 1, 2023, doi: 10.1038/s41598-023-46728-2.

[27] R. G. Jalu, T. A. Chamada, and D. R. Kasirajan, "Calcium oxide nanoparticles synthesis from hen eggshells for removal of lead (Pb(II)) from aqueous solution," Environmental Challenges, vol. 4, 2021, doi: 10.1016/j.envc.2021.100193.

[28] S. J. Lee, H. Jang, and D. N. Lee, "Recent advances in nanoflowers: compositional and structural diversification for potential applications," Nanoscale Advances, vol. 5, no. 19, pp. 5165–5213, 2023, doi: 10.1039/D3NA00163F.

[29] M. Ikram et al., "Synthesis of Al/starch co-doped in CaO nanoparticles for enhanced catalytic and antimicrobial activities: experimental and DFT approaches," RSC Advances, vol. 12, no. 50, 2022, doi: 10.1039/d2ra06340a.

[30] I. K. Abbas and K. A. Aadim, "Synthesis and study of structural properties of calcium oxide nanoparticles produced by laser-induced plasma and its effect on antibacterial activity," Science and Technology Indonesia, vol. 7, no. 4, 2022, doi: 10.26554/sti.2022.7.4.427-434.

[31] R. Eram et al., "Cellular investigations on mechanistic biocompatibility of green synthesized calcium oxide nanoparticles with Danio rerio," Journal of Nanotheranostics, vol. 2, no. 1, 2021, doi: 10.3390/jnt2010004.

[32] S. V. Gudkov, D. E. Burmistrov, D. A. Serov, M. B. Rebezov, A. A. Semenova, and A. B. Lisitsyn, "A mini review of antibacterial properties of ZnO nanoparticles," Frontiers in Physics, vol. 9, 2021, doi: 10.3389/fphy.2021.641481.

[33] A. O. Flayyih, W. K. Mahdi, Y. I. M. Abu Zaid, and F. H. Musa, "Biosynthesis, characterization, and applications of bismuth oxide nanoparticles using aqueous extract of Beta vulgaris," Chemical Methodologies, vol. 6, no. 8, pp. 620–628, 2022, doi: 10.22034/chemm.2022.342124.1522.

[34] C. Huang et al., "Effects of water deficit at different stages on growth and ear quality of waxy maize," Frontiers in Plant Science, vol. 14, 2023, doi: 10.3389/fpls.2023.1069551.

[35] M. Abd Elhakem, W. Botras, A. Hassan, and E. Adly, "Effect of drought stress on growth and productivity of some Mentha species," Scientific Journal of Agricultural Sciences, vol. 5, no. 2, 2023, doi: 10.21608/sjas.2023.211303.1304.

[36] Z. Yang and F. Qin, "The battle of crops against drought: genetic dissection and improvement," Journal of Integrative Plant Biology, vol. 65, no. 2, 2023, doi: 10.1111/jipb.13451.

[37] M. Cooper and C. D. Messina, "Breeding crops for drought-affected environments and improved climate resilience," The Plant Cell, vol. 35, no. 1, pp. 162–186, 2023, doi: 10.1093/plcell/koac321.

[38] H. T. Ebeed, N. M. Hassan, and H. S. Ahmed, "Silicon-mediated improvement of drought tolerance in two wheat genotypes," Egyptian Journal of Botany, vol. 63, no. 2, 2023, doi: 10.21608/ejbo.2023.169059.2169.

[39] R. Mittler, S. I. Zandalinas, Y. Fichman, and F. Van Breusegem, "Reactive oxygen species signalling in plant stress responses," Nature Reviews Molecular Cell Biology, 2022, doi: 10.1038/s41580-022-00499-2.

[40] A. Raza et al., "Nano-enabled stress-smart agriculture: can nanotechnology deliver drought and salinity-smart crops?" Smart Agricultural Technology, 2023, doi: 10.1002/sae2.12061.

[41] M. W. Mazhar et al., "Seed nano-priming with calcium oxide maintains the redox state by boosting the antioxidant defense system in water-stressed carom (Trachyspermum ammi L.) plants to confer drought tolerance," Nanomaterials, vol. 13, no. 9, 2023, doi: 10.3390/nano13091453.